Inorganic Chemistry

Article

pubs.acs.org/IC

Mechanisms for the Reactions of Group 10 Transition Metal Complexes with Metal−Group 14 Element Bonds, Bbt(Br)E═M(PCy_3)$_2$ (E = C, Si, Ge, Sn, Pb; M = Pd and Pt)

Wei-Hung Liao, Pei-Yun Ho, and Ming-Der Su*

Department of Applied Chemistry, National Chiayi University, Chiayi 60004, Taiwan

Supporting Information

ABSTRACT: The electronic structures of the Bbt(Br)E═M(PCy_3)$_2$ (E = C, Si, Ge, Sn, Pb and M = Pt, Pd) complexes and their potential energy surfaces for the formation and water addition reactions were studied using density functional theory (B3LYP/LANL2DZ). The theoretical evidence suggests that the bonding character of the E═M double bond between the six valence-electron Bbt(Br)E: species and the 14 valence-electron (PCy_3)$_2$M complexes has a predominantly high s-character. That is, on the basis of the NBO, this theoretical study indicates that the σ-donation from the E element to the M atom prevails. Also, theoretical computations suggest that the relative reactivity decreases in the order: Bbt(Br)C═M(PCy_3)$_2$ > Bbt(Br)Si═M(PCy_3)$_2$ > Bbt(Br)Ge═M(PCy_3)$_2$ > Bbt(Br)Sn═M(PCy_3)$_2$ > Bbt(Br)Pb═M(PCy_3)$_2$, irrespective of whether M = Pt or M = Pd is chosen. Namely, the greater the atomic weight of the group 14 atom (E), the larger is the atomic radius of E and the more stable is its Bbt(Br)E═M(PCy_3)$_2$ doubly bonded species toward chemical reactions. The computational results show good agreement with the available experimental observations. The theoretical results obtained in this work allow a number of predictions to be made.

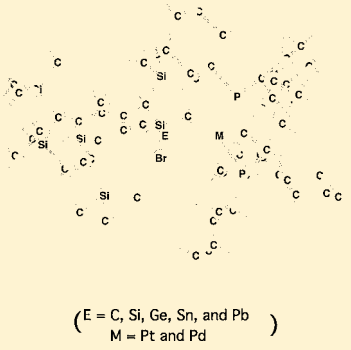

I. INTRODUCTION

The coordination chemistry of the heavier analogues of R_2E: carbenes (E = C, Si, Ge, Sn, and Pb) has attracted enormous research interest in the past few decades, because of their potential role as ligands for transition metals and their hypothetical role in many catalytic processes.[1,2] It has been found that the characteristics of the R_2E: species, which serve as σ-donors and π-acceptors toward transition metal centers, can be varied by adjusting by the nature of the substituents R.[3] As a result, many interesting carbene-like transition metal complexes of the type, $R_2C{=}ML_n$, have been synthesized and characterized to date.[1] Although many attempts have been made, the availability of stable heavier $R_2E{=}ML_n$ complexes remains limited, especially that of the heavy carbonic moieties, owing to the difficulty of preparation of an appropriate heavy carbene ligand source.

Only very recently, the elegant studies performed by Agou, Sasamori and Tokitoh isolated Bbt(Br)Si═Pt(PCy_3)$_2$ (Bbt = 2,6-bis[bis(trimethylsilyl)methyl]-4-[tris(trimethylsilyl)-methyl]phenyl and Cy = cyclohexane),[4] which represents the first example of an arylbromosilylene-platinum complex that uses a 1,2-dibromosilene as a silylene source (see Scheme 1). Details of its conformation concern its synthesis and X-ray structure.[4] It was also found that this new molecular species is air- and moisture-sensitive.[4] However, as far as the authors are aware, no detailed mechanisms for its reactions have been reported, either experimentally or theoretically.

It is this fascinating experimental breakthrough that has inspired this study. If a stable silylene-group 10 transition metal complex can be synthesized and isolated, it should be possible to extrapolate this feature to other molecular systems containing either E═Pd or E═Pt double bonds.[5] As stated above, no quantum chemical computations for the reactions of Bbt(Br)Si═Pt(PCy_3)$_2$ have yet been performed, let alone a systematic theoretical study of elemental effects on the

Scheme 1

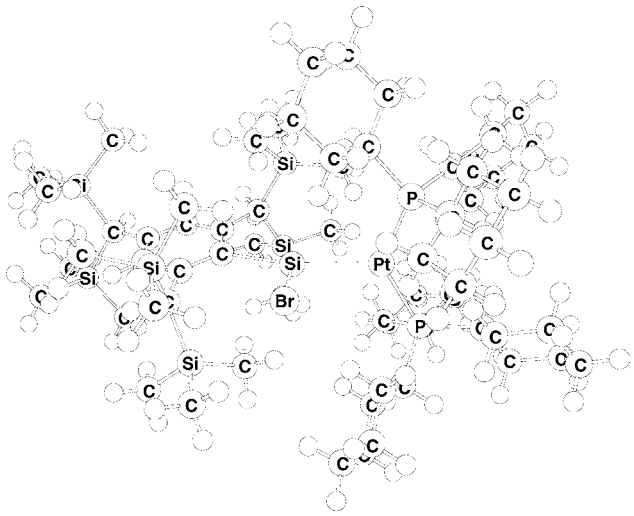

Received: September 18, 2012
Published: January 22, 2013

   dx.doi.org/10.1021/ic302031f | Inorg. Chem. 2013, 52, 1338−1348

reactivity of molecules with either E═Pd or E═Pt double bonds.

$$Bbt(Br)E{=}E(Bbt)Br \rightarrow 2Bbt(Br)E: \quad (1)$$

$$Bbt(Br)E: + (PCy_3)_2M \rightarrow Bbt(Br)E{=}M(PCy_3)_2 \quad (2)$$

$$Bbt(Br)E{=}Pt(PCy_3)_2 + H_2O \rightarrow Bbt(Br)(H)E - Pt(OH)(PCy_3)_2 \quad (3a)$$

$$Bbt(Br)E{=}Pt(PCy_3)_2 + 2H_2O \rightarrow Bbt(Br)(H)E - Pt(OH)(PCy_3)_2 + H_2O \quad (E = C, Si, Ge, Sn, Pb \text{ and } M = Pd, Pt) \quad (3b)$$

This study aims to reach a more thorough understanding of carbene-like transition metal complex chemistry. A density functional theory (DFT) study is presented that investigates the electronic structures of $Bbt(Br)E{=}M(PCy_3)_2$ and Bbt-(Br)E═E(Br)(Bbt) (E = C, Si, Ge, Sn and Pb; M = Pd and Pt) and the mechanisms of their chemical reactions (see eqs 1−3).[6] It is believed that, in view of the recent dramatic developments in stable heavy carbene-transition-metal complex chemistry,[1−5] the results obtained in this work allow the prediction of a reaction pathway for some known and/or as yet unknown systems and allow optimal designs for synthesis and catalysis in doubly bonded carbene-like transition metal complex chemistry.

II. THEORETICAL METHODS

All geometries were fully optimized, without imposing any symmetry constraints, although in some instances the resulting structure showed various elements of symmetry. The DFT calculations used the hybrid gradient-corrected exchange functional proposed by Becke,[7] combined with the gradient-corrected correlation functional of Lee, Yang and Parr.[8] This functional theory is commonly known as B3LYP and has been shown to be quite reliable both for geometries and energies.[9] These B3LYP calculations were performed with relativistic effective core potentials on group 14 elements modeled using the double-ζ (DZ) basis sets[10] augmented by a set of d-type polarization functions.[11] Accordingly, these B3LYP calculations are denoted as B3LYP/LANL2DZ. It is noteworthy that the model reactant ($Bbt(Br)Si{=}Pt(PCy_3)_2$) has a total of 919 (566 electrons) basis functions for the B3LYP/LANL2DZ level of theory. Nature bond orbital (NBO)[12] and Wiberg bond index[13] calculations on the model complexes were performed using the NBO program (Version 3.1) in the GAUSSIAN 03 program package.[14]

Spin-unrestricted (UB3LYP) formalism was used for the open-shell (triplet) species. The S^2 expectation values for the triplet states of the radical products all demonstrated an ideal value (2.00) after spin annihilation, so their geometries and energetics are reliable for this study. Frequency calculations were performed on all structures, in order to confirm that the reactants and products had no imaginary frequencies and that the transition states possessed only one imaginary frequency. The relative energies were thus corrected for vibrational zero-point energies (ZPE, not scaled). The thermodynamic corrections to 298 K, ZPE corrections, heat capacity corrections and entropy corrections (ΔS) obtained were applied at the B3LYP/LANL2DZ level. The relative free energy (ΔG) at 298 K was also calculated at the same level of theory. All of the DFT calculations were performed using the GAUSSIAN 03 package of programs.[14] The optimized geometries for the model complexes are all included in the Supporting Information.

III. RESULTS AND DISCUSSION

A. General Considerations. In order to address the questions which form the basis for this study, a brief examination of the electronic structure of the $R_2E{=}ML_2$ complex is necessary. First, the $R_2E{=}ML_2$ molecule is separated into the R_2E: and ML_2 fragments (see Figure 1). It

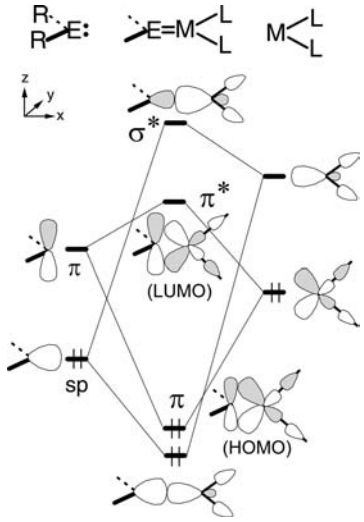

Figure 1. A valence orbital interaction diagram for $R_2E{=}ML_2$.

is well-established that the six valence-electron carbene-like species, R_2E:, has two valence electrons on the R_2E: moiety. These are spin-paired to form a lone pair and occupy an orbital with a predominantly sp-character. This orbital is known as the highest occupied molecular orbital (HOMO). The lowest unoccupied molecular orbital (LUMO) of the R_2E: species is a perpendicular p orbital on the E center.[15] A general outline of the valence molecular orbitals in d^{10} ML_2 has been given previously.[16] Only the two key orbitals, b_2 (HOMO) and $3a_1$ (LUMO), are chosen to be shown on the right side of Figure 1. As a result, the interaction between the valence orbitals of the R_2E: and ML_2 fragments, schematically represented in Figure 1, leads to the MOs of a perpendicular structure $R_2E{=}ML_2$. In other words, the carbene-like-group 10 transition metal complex ($Bbt(Br)E{=}M(PCy_3)_2$) studied in this work prefers to adopt the perpendicular conformation because of its electronic structure, rather than any steric effect due to the substituents (see **1**).

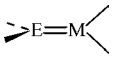

1

Further, as seen in Figure 1, two bonding MOs ($\sigma + \pi$) are produced and four electrons fill these orbitals. It is evident that the atomic coefficients for the two lower levels ($\sigma + \pi$) in Figure 1 are larger than those for the high energy combinations ($\sigma^* + \pi^*$), because of the electronic perturbation effect.[17] That is to say, in the σ orbital, the E sp coefficient is larger than the M $3a_1$ coefficient, while in the π orbital, the E p coefficient is smaller than the M b_2 coefficient. Conversely, in the π^* orbital,

dx.doi.org/10.1021/ic302031f | Inorg. Chem. 2013, 52, 1338−1348

the E p coefficient is larger than the M b_2 coefficient, whereas in σ^* orbital, the E sp coefficient is smaller than the M $3a_1$ coefficient. This electronic structure is used in a later section to explain several phenomena found experimentally.

B. Geometries and Electronic Structures of the Bbt(Br)E═M(PCy$_3$)$_2$ Complexes. Because the structure of Bbt(Br)Si═Pt(PCy$_3$)$_2$ has already been identified using X-ray diffraction,[4] the optimization of its geometry was first performed at the B3LYP level of theory, using the LANL2DZ basis set, in order to test reliability of this method. The key geometrical parameters of Bbt(Br)Si═Pt(PCy$_3$)$_2$ are given in Figure 2, together with some known experimental data.[4] It is

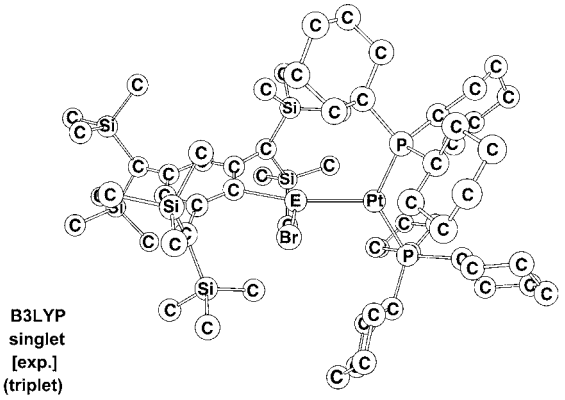

E	C	Si	Ge	Sn	Pb
E – Pt	1.860	2.247 [2.208]	2.377	2.549	2.745
	(2.010)	(2.449)	(2.544)	(2.682)	(2.955)
E – Br	2.261	2.362 [2.314]	2.593	2.742	2.815
	(2.352)	(2.428)	(2.628)	(2.775)	(2.841)
E – C	1.482	1.951 [1.916]	2.062	2.257	2.396
	(1.486)	(1.967)	(2.084)	(2.248)	(2.477)
Pt – E – C	162.2	155.3 [151.9]	162.3	163.3	165.1
	(146.2)	(143.8)	(142.8)	(141.7)	(163.1)
C – E – Br	104.9	102.4 [98.16]	105.6	106.0	107.2
	(110.8)	(110.0)	(110.6)	(111.5)	(112.2)
Br – E – Pt	92.74	102.7 [109.9]	91.80	90.40	87.18
	(101.4)	(88.53)	(86.35)	(85.88)	(83.69)
θ	63	75 [72]	74	76	78
	(71)	(82)	(84)	(86)	(85)

Figure 2. B3LYP/LANL2DZ optimized geometries (in Å and deg) of both singlet and triplet Bbt(Br)E═Pt(PCy$_3$)$_2$ (E = C, Si, Ge, Sn, and Pb) complexes, compared with the available experimental work (ref 4). The definition of the dihedral angle θ (deg); see ref 16. Hydrogens are omitted for clarity.

readily seen that there is agreement between the calculated and experimental values for the Si═Pt, Si–Br and Si–C bond distances, as well as for the ∠C–Si–Br, ∠Br–Si–Pt and θ[18] bond angles, with a variation of 0.049 Å in bond length and 7.2° in bond angle. The discrepancies in these bond angles may be due to the packing force in the crystal structure. Although it would be desirable to perform these computations using an even higher level of theory, the constraints imposed by the present molecular size and available CPU time and disk space make this option impracticable. Nevertheless, because of the reasonable agreement between the B3LYP/LANL2DZ results and the available experimental values,[4] it is expected that the same relative accuracy should also apply to the predicted geometries and energetics for the other doubly bonded Bbt(Br)E═M(PCy$_3$)$_2$ (E = group 14 elements; M = Pd and Pt) species.

Figure 2 shows that the E═Pt double bond distance for both singlet and triplet states demonstrates a monotonic increase down the group, from C to Pb. Also, regardless of multiplicity, both the E–Br and E–C bond lengths show a monotonic increase from E = C to E = Pb. This occurs mainly because of the increase in atomic radius of E, from carbon to lead. These theoretical investigations also indicate that both the E═Pt and E–Br distances are larger for the singlet than for the equivalent triplet species, while the bond angle ∠Pt–E–C is smaller for the singlet than for its corresponding triplet. The computations indicate that all the Bbt(Br)E═Pt(PCy$_3$)$_2$ complexes adopt a staggered conformation, with the Bbt(Br)E: and (PCy$_3$)$_2$Pt fragments being positioned almost orthogonal to each other, mainly because of the effect of the electronic structure, rather than the steric effects, as previously noted (see **1**). Similar optimized geometries and key valence bond orbitals for the other Bbt(Br)E═Pd(PCy$_3$)$_2$ (E = C, Si, Ge, Sn and Pb) species are given in the Supporting Information (Figures A and B, respectively). Basically, the theoretical findings for the optimized geometries and electronic structures of the Bbt(Br)-E═Pd(PCy$_3$)$_2$ complexes are analogous to those for the Bbt(Br)E═Pt(PCy$_3$)$_2$ species.

In order to gain a better understanding of the nature of the chemical bonding in the series of Bbt(Br)E═Pt(PCy$_3$)$_2$ molecules, their selected valence MOs, based on the B3LYP/LANL2DZ calculations, are presented in Figure 3. For convenience, only four key orbitals (σ, π, π^*, and σ^*) of the Bbt(Br)E═Pt(PCy$_3$)$_2$ species are selected to be shown in Figure 3, similar to Figure 1. First, the electronic character of the Si–Pt bond of the model complex (Bbt(Br)Si═Pt(PCy$_3$)$_2$) is compared with the previous calculations.[4] As seen in Figure 3, the HOMO and HOMO-1 of Bbt(Br)Si═Pt(PCy$_3$)$_2$ correspond to the σ- and π-type bonding orbitals, which are basically sp type and p-d type orbitals, respectively. Additionally, these orbitals contain small contributions from the Si–Br σ^* antibonding orbitals. The LUMO of Bbt(Br)Si═Pt(PCy$_3$)$_2$ corresponds to the Si–Pt π^* antibonding orbital, which mainly consists of the vacant Si (3p) orbital with a smaller contribution from the occupied b_2 orbital of the Pt(PCy$_3$)$_2$ moiety. Finally, the Si═Pt σ^* antibonding orbital is located in the higher energy level. The interactions between the silicon center of the Bbt(Br)Si unit and the Pt center of the (PCy$_3$)$_2$Pt fragment were further analyzed on the basis of the NBO calculations.[12] See Table 1. The B3LYP results demonstrate that the NBO of the Si═Pt bonding interaction is as follows: BD(Si–Pt) = 0.8762(3s3p$^{0.73}$)Si + 0.4817(6s6p$^{0.33}$)Pt. This implies that the predominant bonding interaction between the Bbt(Br)Si unit and the (PCy$_3$)$_2$Pt moiety originates from the 3σ(Si) → 6σ^*(Pt) σ-donation. Further supporting evidence for this observation comes from the fact that the Wiberg bond index[13] of the Si–Pt bond in Bbt(Br)Si═Pt(PCy$_3$)$_2$ is 1.323, which suggests that this Si–Pt bond is best described as a single bond, rather than a traditional double bond. In principle, these analyses of the electronic structure are consistent with those of Agou, Sasamori and Tokitoh.[4]

Table 1 also shows a population analysis for the other singlet Bbt(Br)E═Pt(PCy$_3$)$_2$ species, based on the NBO values[12] and on the Wiberg bond indices.[13] Similar theoretical bonding properties for the Bbt(Br)E═Pd(PCy$_3$)$_2$ molecules are listed

dx.doi.org/10.1021/ic302031f | Inorg. Chem. 2013, 52, 1338–1348

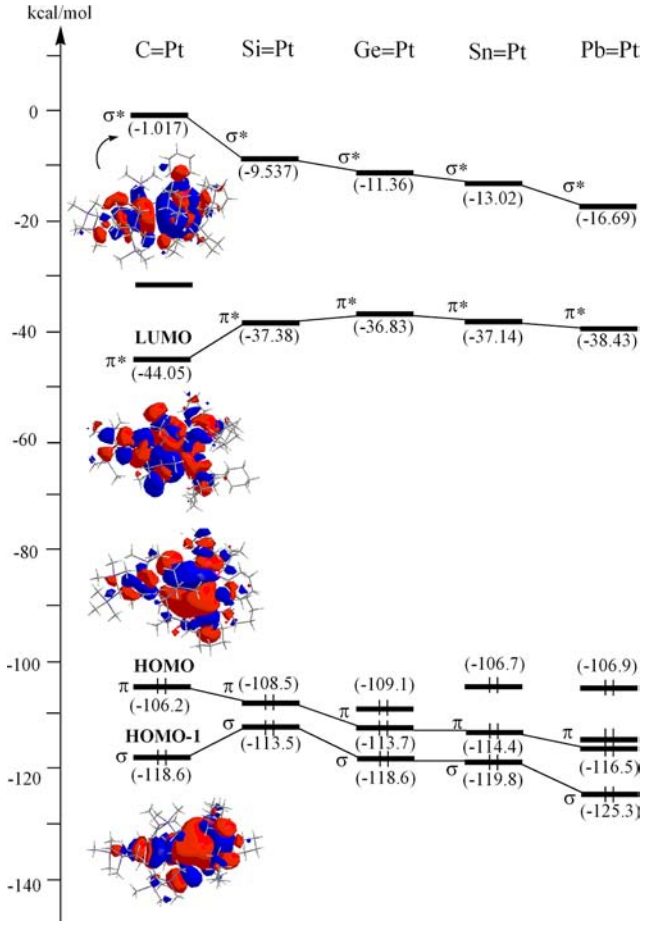

Figure 3. Calculated key molecular orbital for the singlet Bbt(Br)E═Pt(PCy_3)$_2$ (E = C, Si, Ge, Sn, and Pb) species. For more information see Figure 1 and the text.

Table 1. Bonding Properties Based on the NBO Values and on the Wiberg Bond Indices for Bbt(Br)E═Pt(PCy_3)$_2$ (E = C, Si, Ge, Sn, and Pb) at the B3LYP/LANL2DZ Level of Theory

(1) Bbt(Br)C═Pt(PCy_3)$_2$	
C−Pt hybrids	C: 29.88% (0.01% s and 99.99% p)
	Pt: 70.12% (0.03% p and 99.96% d)
Wiberg bond order	C−Pt: 1.323
(2) Bbt(Br)Si═Pt(PCy_3)$_2$	
Si−Pt hybrids	Si: 68.18% (66.18% s and 30.25% p)
	Pt: 44.72% (72.37% s and 25.54% p)
Wiberg bond order	Si−Pt: 0.9223
(3) Bbt(Br)Ge═Pt(PCy_3)$_2$	
Ge−Pt hybrids	Ge: 65.92% (66.20% s and 29.62% p)
	Pt: 39.02% (71.04% s and 24.01% p)
Wiberg bond order	Ge−Pt: 0.8300
(4) Bbt(Br)Sn═Pt(PCy_3)$_2$	
Sn−Pt hybrids	Sn: 62.08% (65.31% s and 23.88% p)
	Pt: 37.02% (65.50% s and 22.08% p)
Wiberg bond order	Sn−Pt: 0.7165
(5) Bbt(Br)Pb═Pt(PCy_3)$_2$	
Pb−Pt hybrids	Pb: 64.98% (61.28% s and 21.78% p)
	Pt: 35.71% (62.47% s and 20.19% p)
Wiberg bond order	Pb−Pt: 0.4894

in the Supporting Information (Table A and Figures A and B). Table 1 shows that the Wiberg bond indices at the B3LYP level are predicted to decrease down the group 14 family, from Bbt(Br)C═Pt(PCy_3)$_2$ to Bbt(Br)pb═Pt(PCy_3)$_2$. This decrease is attributable to the E═Pt double bond distance, since this bond length increases in the order: 1.860 Å (Bbt(Br)C═Pt(PCy_3)$_2$) < 2.247 Å (Bbt(Br)Si═Pt(PCy_3)$_2$) < 2.377 Å (Bbt(Br)Ge═Pt(PCy_3)$_2$) < 2.549 Å (Bbt(Br)Sn═Pt(PCy_3)$_2$) < 2.745 Å (Bbt(Br)Pt═Pt(PCy_3)$_2$).[19]

As schematically shown in Figure 3, the substitution of a single E atom in the Bbt(Br)E═Pt(PCy_3)$_2$ species decreases the energy of the π bonding orbital, on going from C to Pb. This substitution also results in a decrease in the σ bonding orbital energy down the group 14 elements, E, especially for the heaviest Bbt(Br)Pb═Pt(PCy_3)$_2$ complex. The locations of these molecular orbitals are attributable to a relativistic effects, also known as the "orbital non-hybridization effect" and "inert s-pair effect", as discussed earlier.[20] Figure 3 shows that after the E substitution, the energy of the π^* antibonding orbital increases along the series, from Bbt(Br)C═Pt(PCy_3)$_2$ to Bbt(Br)Pb═Pt(PCy_3)$_2$. It is interesting that these π^* antibonding orbitals are always LUMOs. Further, one important feature of the Bbt(Br)E═Pt(PCy_3)$_2$ complex is its singlet−triplet splitting ΔE_{st} (= $E_{triplet}$ − $E_{singlet}$). This study's DFT calculations indicate that the ΔE_{st} for the molecules containing the C═Pt, Si═Pt, Ge═Pt, Sn═Pt, and Pb═Pt double bond is 62.1, 71.1, 76.9, 77.3, and 78.1 kcal/mol, respectively. In other words, the heavier the group 14 atom (E), the larger is the ΔE_{st} of Bbt(Br)E═Pt(PCy_3)$_2$. This occurs mainly because the magnitude of the energy difference between π and π^* for the Bbt(Br)E═Pt(PCy_3)$_2$ systems becomes larger, from C to Pb, due to relativistic effects,[20] as stated above. Accordingly, these theoretical findings indicate that the electronic perturbation effect, wherein the heavier group 14 element E changes, plays a dominant role in determining the energy ordering of the frontier orbitals. This, in turn, affects the magnitude of the ΔE_{st} for these E═Pt and E═Pd doubly bonded complexes.

The factors responsible for the difference in the reactivity of the Bbt(Br)E═Pt(PCy_3)$_2$ (E = C, Si, Ge, Sn and Pb) complexes are of interest. Figure 3 shows that the HOMO and LUMO energy levels of Bbt(Br)E═Pt(PCy_3)$_2$ for molecules possessing the C═Pt, Si═Pt, Ge═Pt, Sn═Pt, and Pb═Pt double bond are (kcal/mol): (−106, −44.1), (−109, −37.4), (−109, −36.8), (−107, −37.1), and (−107, −38.4), respectively. If the reactions were "frontier-orbital-controlled", a more facile reaction would be seen for Bbt(Br)Pb═Pt(PCy_3)$_2$ than for Bbt(Br)Si═Pt(PCy_3)$_2$ or Bbt(Br)Ge═Pt(PCy_3)$_2$. As will be shown in the subsequent section, this is not the case. The relative reactivity of these species is readily identified on the basis of the relative values of ΔE_{st} for Bbt(Br)Si═Pt(PCy_3)$_2$ complexes. Apparently, the lower reactivity of Bbt(Br)E═Pt(PCy_3)$_2$ with a group 14 element, E, of a heavier atomic weight is due to its higher ΔE_{st} (vide infra). Indeed, the stability of the carbene-like transition metal complexes is determined by the ΔE_{st} of Bbt(Br)E═Pt(PCy_3)$_2$. If the ΔE_{st} is small, the Bbt(Br)E═Pt(PCy_3)$_2$ molecules are unstable and easily undergo facile chemical reactions (such as with solvents, etc.). As already shown in Figure 3, the theoretical calculations demonstrate that the Bbt(Br)E═Pt(PCy_3)$_2$ complexes have comparatively large singlet−triplet separations (ΔE_{st} > 62 kcal/mol). Accordingly, the large ΔE_{st} in such Bbt(Br)E═Pt(PCy_3)$_2$ doubly bonded molecules strongly implies that

dx.doi.org/10.1021/ic302031f | Inorg. Chem. 2013, 52, 1338−1348

these species should be stable enough to be detected experimentally. Supporting evidence for this observation comes from the fact that, so far, a silicon−platinum complex with a Si═Pt double bond (i.e., Bbt(Br)Si═Pt(PCy_3)$_2$) has been experimentally isolated and characterized.[4] It should emphasized here that these phenomena are also seen in the Bbt(Br)E═Pd(PCy_3)$_2$ complexes. That is to say, this study's DFT calculations demonstrate that the ΔE_{st} and the stability of the Bbt(Br)E═Pd(PCy_3)$_2$ species increases in the order: C═Pd < Si═Pd < Ge═Pd < Sn═Pd < Pb═Pd, whose data are given in Supporting Information.

C. Geometries and Electronic Structures of the Bbt(Br)E═E(Bbt)Br System. The geometries and electronic structures of Bbt(Br)E═E(Bbt)Br compounds that possess a E═E double bond (E = C, Si, Ge, Sn, and Pb) are now examined. These were calculated in both singlet and triplet states at the B3LYP/LANL2DZ level of theory, and their selected geometrical parameters are shown in Figure 4.

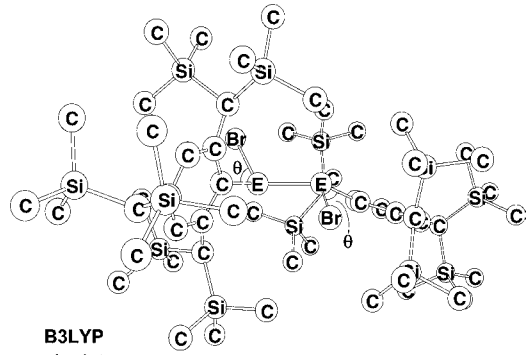

E	C	Si	Ge	Sn	Pb
E = E	1.389	2.372	2.852	3.193	3.366
	(1.488)	(2.667)	(2.920)	(3.235)	(3.377)
E − Br	2.006	2.421	2.558	2.694	2.761
	(2.053)	(2.419)	(2.518)	(2.677)	(2.772)
E − C	1.556	1.927	1.993	2.166	2.217
	(1.492)	(1.937)	(2.032)	(2.193)	(2.316)
θ	110.4	107.4	105.4	106.2	107.3
	(113.7)	(107.9)	(108.2)	(110.1)	(110.5)
ϕ	2.231	41.25	48.51	51.40	52.11
	(25.09)	(46.11)	(48.46)	(52.72)	(56.39)

Figure 4. B3LYP/LANL2DZ optimized geometries (in Å and deg) of both singlet and triplet Bbt(Br)E═E(Bbt)Br (E = C, Si, Ge, Sn, and Pb) molecules. The definition of the dihedral angle θ (deg); see **2**. Relative energies for each species; see Table 2. Hydrogens are omitted for clarity.

The DFT calculations shown in Figure 4 indicate that the calculated E═E double bond length in the singlet Bbt(Br)E═E(Bbt)Br species increases in the order: 1.389 Å (C═C) < 2.372 Å (Si═Si) < 2.852 Å (Ge═Ge) < 3.193 Å (Sn═Sn) < 3.366 Å (Pb═Pb). It has been shown experimentally that the E═E double bond lengths are 1.356 Å (C═C),[21] 2.139−2.360 Å (Si═Si),[22] 2.212−2.509 Å (Ge═Ge),[23] 2.601−2.961 Å (Sn═Sn),[24] and 2.990−3.537 Å (Pb═Pb).[25] Indeed, Tokitoh and many co-workers have synthesized and structurally characterized Bbt(Br)Si═Si(Bbt)Br[22c] and Bbt(Br)Ge═Ge(Bbt)Br.[23d] They reported the experimental double bond lengths are 2,226 Å (Si═Si) and 2.509 Å (Ge═Ge), respectively. Apparently, the singlet C═C, Si═Si, Ge═Ge, Sn═Sn, and Pb═Pb double bond distances presented in this work are somewhat larger than the experimentally reported data,[20−25] bearing in mind that the molecules used for calculations contain extremely bulky Bbt substituents.

As seen in Figure 4, regardless of the multiplicity adopted by the group 14 Bbt(Br)E═E(Bbt)Br, the B3LYP computations suggest that the E═E bond distance shows a monotonic increase down the group, from C to Pb. The same phenomenon is also seen for the other E−Br and E−C bond lengths. This is simply explained by the increase in the atomic radius of E, from C to Pb. An interesting trend shown in Figure 4 is the increase in the central bond distance, E═E, on going from the singlet to the triplet state. This can be explained by considering the electronic structures (vide infra).

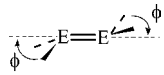

2

The DFT calculations show that the Bbt(Br)C═C(Bbt)Br molecule adopts a nearly planar geometry with an out-of-plane angle ϕ = 2.2° (see **2**). However, the other heavier Bbt(Br)E═E(Bbt)Br compounds have a trans-bent structure with an out-of-plane angle ϕ = 41°, 49°, 51°, and 52°, for Bbt(Br)Si═Si(Bbt)Br, Bbt(Br)Ge═Ge(Bbt)Br, Bbt(Br)Sn═Sn(Bbt)Br and Bbt(Br)Pb═Pb(Bbt)Br, respectively. That is to say, the greater the atomic number of the main group 14 element, E, the greater the out-of-plane angle, ϕ. It has to be noted that Tokitoh and many co-workers reported the out-of-plane angle ϕ = 32.4° and 44.6° for Bbt(Br)Si═Si(Bbt)Br[22c] and Bbt(Br)Ge═Ge(Bbt)Br,[23d] respectively. As a result, our computational values for ϕ about both Bbt(Br)Si═Si(Bbt)Br and Bbt(Br)Ge═Ge(Bbt)Br compounds are a little bit larger than the experimental data. The reason for this could be due to the small basis set (LANL2DZ) used in the present work. In fact, it is well documented that the heavier analogues of the olefins ($R_2E═ER_2$) do not exhibit classical planar geometry, but have a trans-bent structure, with pyramidalization of both R_2E: groups (**2**).[26,27] These compounds, containing so-called "nonclassical double bonds", have been proven to be the preferred arrangements and are local minima on the potential energy surface of all of the heavier analogues of ethylene, from Si_2H_4 to Pb_2H_4. Again, the out-of-plane angles in these heavy ethylene analogues being far from 0° (planar) provide evidence for the core-like nature of the ns (n = 3−6) electrons, that is, the so-called "inert s-pair effect",[20] discussed earlier. Excellent reviews are available in ref 27.

In principle, all of the group 14 Bbt(Br)E═E(Bbt)Br molecules have a two atomic orbital π system, containing two π electrons, in common, This is analogous to an ethylene species, of which the valence MOs based on the B3LYP/LANL2DZ calculations are outlined in Figure 5. As stated previously, the reason for the increase in the E═E bond distance, on going from the singlet to the triplet state, is simply explained by considering the electronic structures of the two states (HOMO and LUMO). As expected, the theoretical results based on the DFT calculations indicate that all of the doubly bonded Bbt(Br)E═E(Bbt)Br possess a singlet ground state. Figure 5 also shows that the HOMO−LUMO energy gap for Bbt(Br)-E═E(Bbt)Br decreases as the atomic number of the group 14 atom (E) increases. This strongly implies that its corresponding singlet−triplet energy splitting ΔE_{st} (= $E_{triplet} - E_{singlet}$) should also decrease as the central E atom becomes heavier. Indeed, this prediction is in accordance with the B3LYP calculations.

dx.doi.org/10.1021/ic302031f | Inorg. Chem. 2013, 52, 1338−1348

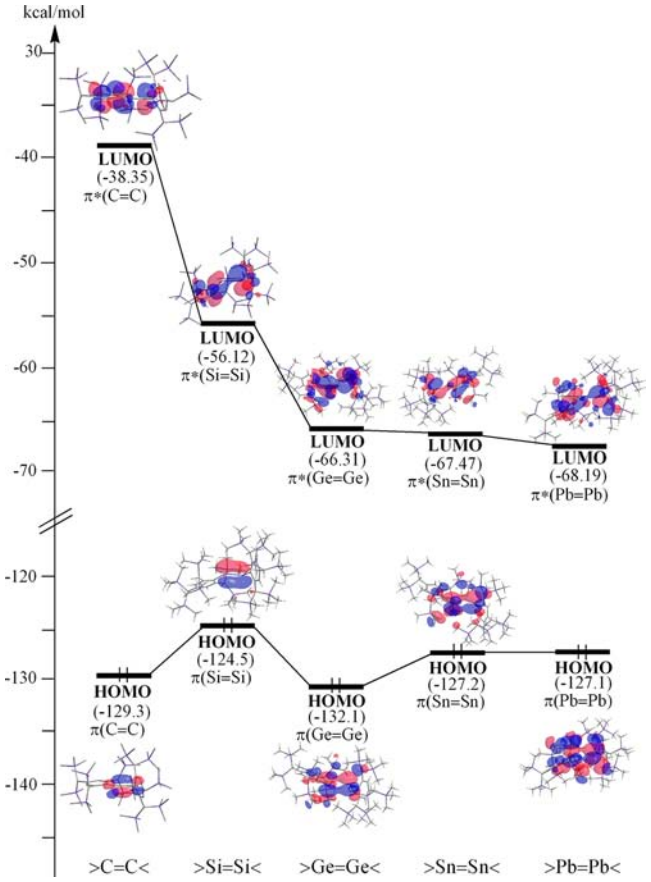

Figure 5. Calculated key molecular orbital for the singlet Bbt(Br)E═E(Bbt)Br (E = C, Si, Ge, Sn, and Pb) species. For more information see the text.

For instance, the Gibbs free ΔE_{st} (kcal/mol) results decrease as follows: +28 (Bbt(Br)C═C(Bbt)Br) > +27 (Bbt(Br)Si═Si(Bbt)Br) > +25 (Bbt(Br)Ge═Ge(Bbt)Br) > +24 (Bbt(Br)-Sn═Sn(Bbt)Br) > +15 (Bbt(Br)Pb═Pb(Bbt)Br). Again, the reason for this can be explained using basic MO theory.[28] Namely, the distortion from planar to trans-bent in a 12-valence-electron >E═E< system results in a decrease in the HOMO and LUMO energy gap, because of a second-order Jahn−Teller effect. See **3**. This, in turn, leads to a decrease in the ΔE_{st} of the >E═E< species, on descending a column of the Periodic Table. As mentioned earlier, because of a lack of experimental and theoretical data for these doubly bonded Bbt(Br)E═E(Bbt)Br species, the computed values presented in this work must be considered as predictions for future investigations.

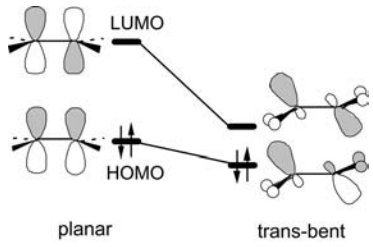

3

D. The Double Bond Dissociations of the Bbt(Br)E═E(Bbt)Br Systems. The dissociation process for the separation of the doubly bonded Bbt(Br)E═E(Bbt)Br molecules into two Bbt(Br)E: monomers is examined. In fact, all currently known compounds, $R_2Sn{=}SnR_2$ and $R_2Pb{=}PbR_2$, as well as many $R_2Ge{=}GeR_2$ species, have E═E doubly bonded dimeric structures in the solid state, but dissociate in solution to yield two monomers, such as R_2Sn:, R_2Pb: and R_2Ge:, respectively. That is, a dimer−monomer equilibrium can exist in solution, as given by eq 4.[29] These experimental findings strongly indicate that the bonding between these elements is relatively weak.[30]

$$R_2E{=}ER_2 \rightleftarrows 2R_2E: \quad (E = Ge, Sn, \text{and } Pb;\ R = \text{large organic ligand}) \tag{4}$$

The mechanism for the dissociation reaction in the Bbt(Br)E═E(Bbt)Br → 2Bbt(Br)E: (eq 1) process was calculated. However, repeated attempts to find a transition state for the concerted dissociation of the Bbt(Br)E═E(Bbt)Br species using the DFT methodology always failed. These theoretical investigations therefore suggest that no transition states exist on the B3LYP/LANL2DZ surface for the dissociation of group 14 Bbt(Br)E═E(Bbt)Br (E = C, Si, Ge, Sn and Pb). Nevertheless, the B3LYP results demonstrate that the Gibbs free dissociation energy of the doubly bonded Bbt(Br)E═E(Bbt)Br species is −16 (C═C), −20 (Si═Si), −23 (Ge═Ge), −24 (Sn═Sn), and −26 (Pb═Pb) kcal/mol. That is, the theoretical results predict that, with due consideration of the thermodynamic factors, the total energy of the two separated monomers is still less than that of the doubly bonded reactant. Presumably, because of steric interactions by the bulky substituents, this theoretical evidence demonstrates that these E═E double bonds are easily broken. As a result, these doubly bonded compounds can readily dissociate into two monomers, either in solution or at room temperature. Indeed, the theoretical conclusions are in good agreement with the available experimental observations. It has been reported that 1,2-dibromodisilene (Bbt(Br)Si═Si(Bbt)-Br)[4,22c] and 1,2-dibromodigermene (Bbt(Br)Ge═Ge(Bbt)-Br)[23d] easily separates to form two units (Bbt(Br)Si: and Bbt(Br)Ge:, respectively), which provide an isolable source of arylbromosilylene, with the proper choice of reaction conditions and partners.[31]

It is worth noting that the theoretical results for the trend of the dissociation energy of Bbt(Br)E═E(Bbt)Br mirror the trend in the singlet−triplet energy splitting ΔE_{st}. That is, the greater the atomic number of the group 14 element, E, in the Bbt(Br)E═E(Bbt)Br molecule, the smaller is its singlet−triplet energy separation ΔE_{st}, the easier its E═E double bond is broken and, in turn, the quicker is its dissociation into two Bbt(Br)E: monomers.

E. The Formation Reactions of the Bbt(Br)E═M$(PCy_3)_2$ Complexes. This section examines the formation mechanisms for doubly bonded Bbt(Br)E═M$(PCy_3)_2$ compounds containing the 6 valence-electron Bbt(Br)E: and the 14 valence-electron d^{10} M$(PCy_3)_2$ units, calculated at the B3LYP/LANL2DZ level of theory (see eq 2). The corresponding relative energies at the DFT level are listed in Table 2.

As predicted, a double-bond between the group 14 atom, E, and the group 10 metal element, M, should form during the reaction for the formation of Bbt(Br)E═M$(PCy_3)_2$. However, repeated searches for the transition state for a product containing Bbt(Br)E: and $(PCy_3)_2$M moieties, using the B3LYP methodology, were always unsuccessful. These theoretical investigations therefore suggest that no transition

dx.doi.org/10.1021/ic302031f | Inorg. Chem. 2013, 52, 1338−1348

Table 2. Relative Energies (all in kcal/mol) for (I) Singlet and Triplet 6 Valence-Electron Bbt(Br)E: and for the Processes: (II) 2Bbt(Br)E: + 2$(PCy_3)_2$Pt → Bbt(Br)E═Pt$(PCy_3)_2$ and (III) 2Bbt(Br)E: + 2$(PCy_3)_2$Pd → Bbt(Br)E═Pd$(PCy_3)_2$[a,b]

(I) system	E = C	E = Si	E = Ge	E = Sn	E = Pb
ΔE_{st} (Bbt(Br)E:)	+3.03 (+3.39)	+27.8 (+26.0)	+30.0 (+34.2)	+36.0 (+37.0)	+42.8 (+44.2)
(II) system	E = C	E = Si	E = Ge	E = Sn	E = Pb
ΔH (Bbt(Br)E═Pt$(PCy_3)_2$)	+12.7 (+20.4)	+9.02 (+6.60)	+16.8 (+8.32)	+26.2 (+9.09)	+28.6 (+10.3)
(III) system	E = C	E = Si	E = Ge	E = Sn	E = Pb
ΔH (Bbt(Br)E═Pd$(PCy_3)_2$)	+19.7 (+15.7)	+22.3 (+8.80)	+26.7 (+11.0)	+30.7 (+14.3)	+32.3 (+15.3)

[a]At the B3LYP/LANL2DZ level of theory. The B3LYP optimized structures of the stationary points see Figure 2 and Supporting Information. [b]Gibbs free energy and zero-point energy (in parentheses).

states exist on the B3LYP/LANL2DZ surface for the formation reactions for group 14 Bbt(Br)E: carbenes and$(PCy_3)_2$M complexes. In Table 2, the B3LYP free energy results also suggest that the energy of the doubly bonded product, relative to its corresponding pair of units, is +13 (C═Pt), +9.0 (Si═Pt), +17 (Ge═Pt), +26 (Sn═Pt) and +29 (Pb═Pt) kcal/mol and +20 (C═Pd), +22 (Si═Pd), +27 (Ge═Pd), +31 (Sn═Pd) and +32 (Pb═Pd) kcal/mol, respectively. These DFT results thus predict that, with due consideration of the thermodynamic factors, the total energy of the doubly bonded products is greater than that of two separated monomers.

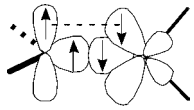

4

The B3LYP computations also demonstrate that the Gibbs free singlet−triplet energy separation, ΔE_{st} (= $E_{triplet} - E_{singlet}$), for the $(PCy_3)_2$Pt and $(PCy_3)_2$Pd fragments are 54 and 66 kcal/mol, respectively. According to the configuration mixing (CM) model of Pross and Shaik,[32,33] the stabilization of the formation product depends on the ΔE_{st} of the reactants (i.e., the $(PCy_3)_2$M complex and the Bbt(Br)E: molecule). That is to say, a smaller ΔE_{st} results in a more stable product, a faster formation reaction and a less endothermic reaction (or a more exothermic reaction). These results show that, if the group 14 element E is a constant, it can be concluded that the Pt reaction is more favorable than the Pd reaction in the formation of the doubly bonded Bbt(Br)E═M$(PCy_3)_2$ complex. This finding is in accordance with the computational data given in Table 2 and with available experimental observations.[4] The reason for the importance of the triplet state in these reactions between group 10 transition metal complexes and group 14 carbenes is as follows (see Figures 1 and 4). Two new chemical bonds ($\sigma + \pi$) must be formed in the product, Bbt(Br)E═M$(PCy_3)_2$, so each $(PCy_3)_2$M and Bbt(Br)E: unit must have at least two open shells and the lowest state of this type is the triplet state. Accordingly, from the valence-bond viewpoint,[32,33] the bonding in the doubly bonded product occurs between the triplet $(PCy_3)_2$M state and the triplet Bbt(Br)E:. As a result, the overall state is singlet. In consequence, if a reactant $(PCy_3)_2$M (or Bbt(Br)E:) molecule has a singlet ground state with a small excitation energy for the triplet state, there is a greater opportunity for the triplet state to take part in the singlet reaction, and bond formation in a single-step is expected to take place more readily. Again, the computed B3LYP results for the Gibbs free ΔE_{st} (kcal/mol) of the Bbt(Br)E: molecules increase in the order: 3.0 (Bbt(Br)C:) < 28 (Bbt(Br)Si:) < 30 (Bbt(Br)Ge:) < 36 (Bbt(Br)Sn:) < 43 (Bbt(Br)Pb:). These computations strongly suggest that if the group 10 metal element M is a constant, the smaller the ΔE_{st} of six valence-electron Bbt(Br)E:, the less endothermic is the reaction, and, in turn, the faster is the formation reaction of the doubly bonded Bbt(Br)E═M$(PCy_3)_2$ complex. This prediction is consistent with the B3LYP computational data for the reaction enthalpies of the Bbt(Br)E═M$(PCy_3)_2$ species, as listed in Table 2.

F. The 1,2-Addition Reactions of the Bbt(Br)E═Pt$(PCy_3)_2$ Complexes with Water. Finally, it is necessary to investigate the mechanisms for the water addition reactions of the Bbt(Br)E═Pt$(PCy_3)_2$ complexes, since it has been reported that the Bbt(Br)Si═Pt$(PCy_3)_2$ compound has been isolated in 56% yield, as moisture- and air-sensitive crystals, by careful recrystallization from the reaction mixture.[4] To the best of the authors' knowledge, there has been no experimental or theoretical study of the mechanisms for the 1,2-addition reactions of heavy carbene-transition-metal complexes with water. As a result, in order to ascertain the factors that control the reactivity of Bbt(Br)E═Pt$(PCy_3)_2$ compounds containing the E═Pt double bond (E = C, Si, Ge, Sn, and Pb), the 1,2-addition of water to these substituted doubly bonded molecules is examined (eq 3). Two possible addition pathways, as shown in **5**, are feasible: one proceeds via monomeric water addition (path 1; eq 3a), while the other proceeds via a dimeric water addition (path 2; path 3b). Figure 6 illustrates the optimized geometries of the reactants (Bbt(Br)E═Pt$(PCy_3)_2$ and H_2O) and the final product (**Pro-E-Pt-H_2O**), together with the transition state (**TS-E-Pt-1H_2O** and **TS-E-Pt-2H_2O**) that connects the reactants and the product. Selected geometrical parameters and relative energies at the B3LYP/LANL2DZ level of theory are summarized in Table 3. The major conclusions to be drawn from this study can be summarized as follows:

dx.doi.org/10.1021/ic302031f | Inorg. Chem. 2013, 52, 1338−1348

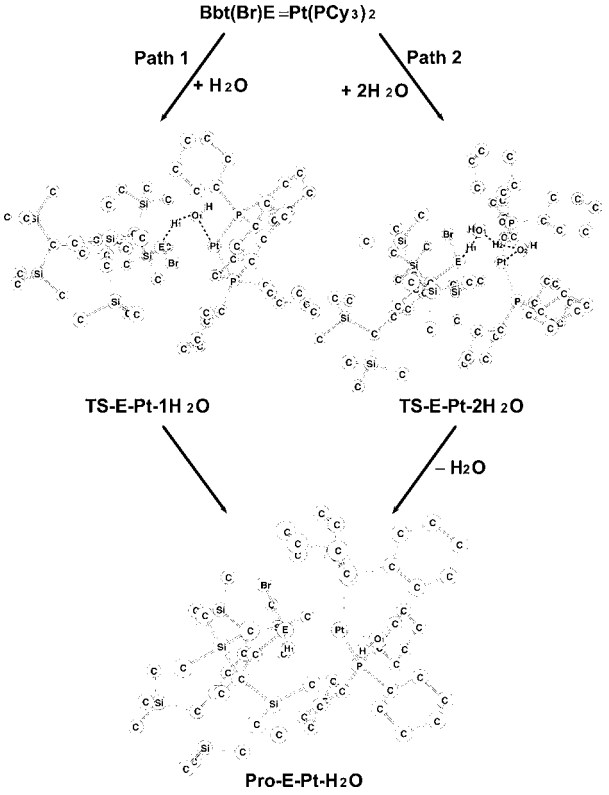

Figure 6. B3LYP/LANL2DZ optimized geometries of the transition states (**TS-E-Pt-H_2O** and **TS-E-Pt-$2H_2O$**) and product (**Pro-E-Pt-H_2O**) for the water addition reaction between reactants Bbt(Br)E=$Pt(PCy_3)_2$ (E = C, Si, Ge, Sn, and Pb) and a H_2O (path 1) or two H_2O (path 2). Selected geometrical parameters and relative energies for each species; see Table 3. Some of hydrogens are omitted for clarity.

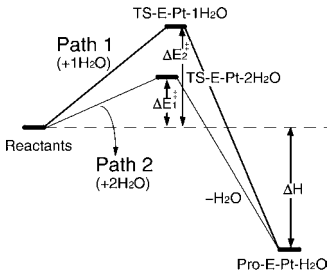

5

For path 1, the transition state (**TS-E-Pt-$1H_2O$**) was located for each of the group 14 elements, E, at the B3LYP level of theory. The DFT frequency calculations for the transition states, **TS-C-Pt-$1H_2O$**, **TS-Si-Pt-$1H_2O$**, **TS-Ge-Pt-$1H_2O$**, **TS-Sn-Pt-$1H_2O$** and **TS-Pb-Pt-$1H_2O$**, suggest that the single values of the imaginary frequencies are 312*i*, 105*i*, 114*i*, 106*i* and 121*i* cm^{-1}, respectively. All of the **TS-E-Pt-$1H_2O$** geometries are quite similar, and they all have a four-center-like structure that includes the E–Pt bond, an oxygen atom and one hydrogen atom from water. These optimized **TS-E-Pt-$1H_2O$** geometries indicate that electrons flow from the lone pair orbital of the oxygen atom into the π^*(E=Pt) antibonding orbital (see Figures 1 and 3). This results in a longer E–Pt bond distance in the **TS-E-Pt-$1H_2O$**. For instance, the theoretical calculations predict distances of 2.361 Å (**TS-C-Pt-$1H_2O$**), 2.617 Å (**TS-Si-Pt-$1H_2O$**), 2.815 Å (**TS-Ge-Pt-$1H_2O$**), 2.878 Å (**TS-Sn-Pt-$1H_2O$**) and 3.033 Å (**TS-Pb-Pt-$1H_2O$**). These theoretical data also show that the heavier the group 14 element, E, involved in the Bbt(Br)E=$Pt(PCy_3)_2$ molecule, the greater is the E–Pt bond length in the **TS-E-Pt-$1H_2O$**. The dimeric water addition pathway (path 2) was also examined, using the same level of theory. The B3LYP frequency calculations for the transition states, **TS-C-Pt-$2H_2O$**, **TS-Si-Pt-$2H_2O$**, **TS-Ge-Pt-$2H_2O$**, **TS-Sn-Pt-$2H_2O$** and **TS-Pb-Pt-$2H_2O$**, predict that the values of the single imaginary frequencies are 99.3*i*, 113*i*, 210*i*, 175*i*, and 94.5*i* cm^{-1}, respectively. Again, because the lone pair of electrons of the oxygen atom interact and are donated to the π^* antibonding orbital of the E=Pt double bond in the **TS-E-Pt-$2H_2O$**, as previously mentioned, their E–Pt bond lengths are expected to be longer than that of the corresponding reactant, as shown in Table 3.

From Table 3, it is obvious that the activation barrier for path 1 is much larger than that for path 2. For instance, the B3LYP free energy results (kcal/mol) demonstrate that 43 (**TS-C-Pt-$1H_2O$**) > 11 (**TS-C-Pt-$2H_2O$**), 54 (**TS-Si-Pt-$1H_2O$**) > 14 (**TS-Si-Pt-$2H_2O$**), 61 (**TS-Ge-Pt-$1H_2O$**) > 18 (**TS-Ge-Pt-$2H_2O$**), 68 (**TS-Sn-Pt-$1H_2O$**) > 39 (**TS-Sn-Pt-$2H_2O$**) and 71 (**TS-Pb-Pt-$1H_2O$**) > 41 (**TS-Pb-Pt-$2H_2O$**). As a consequence, path 2 (dimeric form) is concluded to be preferred to path 1 (monomeric form) for the water 1,2-addition reactions to doubly bonded Bbt(Br)E=$Pt(PCy_3)_2$ complexes. In addition, the computations demonstrate that for both monomeric and dimeric water addition reactions the activation energy increases as the group 14 atom, E, becomes heavier.

As shown in **5**, a comparison of the two pathways for the reaction of the Bbt(Br)E=$Pt(PCy_3)_2$ double bond molecules with H_2O and $2H_2O$ leads to the same products, i.e., **Pro-C-Pt-H_2O**, **Pro-Si-Pt-H_2O**, **Pro-Ge-Pt-H_2O**, **Pro-Sn-Pt-H_2O** and **Pro-Pb-Pt-H_2O**, whose key geometrical parameters are given in Table 3. The DFT computations show that the E–Pt bond distance of the final product is longer than that of the corresponding reactant and that this bond distance increases along group 14, from carbon to lead. More importantly, the B3LYP theoretical results demonstrate that the order of the reaction free enthalpy follows the same trend as that for the activation energy as given in Table 3. That is to say, the lower the atomic number of the group 14 atom (E) in the Bbt(Br)E=$Pt(PCy_3)_2$ reactant, the smaller is the barrier height, the more exothermic is the reaction enthalpy and, in turn, the easier is the water 1,2-addition reaction. In particular, addition reactions with the dimeric form of water have significantly lower barriers than those for monomeric H_2O. It is thus anticipated that the addition of water to the E=Pt double bond of the Bbt(Br)E=$Pt(PCy_3)_2$ reactants should involve a polymeric form (at least the dimeric form) of water, rather than the monomeric form. As there are no relevant experimental or theoretical data for the addition of water to the Bbt(Br)E=$Pt(PCy_3)_2$ systems, the conclusions presented in this work should be considered as predictions for future investigations.

In this theoretical analysis, all of the computational results can be explained using the CM model,[32,33] as stated previously. According to the CM model, the stabilization of the transition state of an addition reaction depends on the singlet–triplet energy splitting ΔE_{st} (= $E_{triplet} - E_{singlet}$) of the Bbt(Br)E=$Pt(PCy_3)_2$ complexes. That is, a smaller ΔE_{st} results in a more stable transition state, lower activation energy and a faster addition reaction with water. The B3LYP computations using the model, shown in Table 3, confirm this prediction. That is to

dx.doi.org/10.1021/ic302031f | Inorg. Chem. 2013, 52, 1338–1348

Table 3. Selected Geometrical Parameters (Bond Distances in Å), Relative Zero-Point Energies (kcal/mol) and Relative Gibbs Free Energies (kcal/mol) at 298 K at the B3LYP/LANL2DZ Level of Theory for the Optimized Stationary Points on the Studied Water 1,2-Addition Channels[a]

	geometrical parameters					energies	
system	E−Pt	Pt−O_1	E−H_1	O_1−H_1	O−H_2	ΔE^b	ΔG
>C=Pt<	1.860					0.00	0.00
TS−C-Pt-1H_2O	2.361	2.311	1.490	1.137		30.21 (99.08) [−68.87]	43.83
TS−C-Pt-2H_2O	2.077	2.874	1.264	1.369	2.224	7.258	11.44
Pro−C−Pt-H_2O	2.182	2.089	1.104	4.063		4.537	−16.53
>Si=Pt<	2.247					0.00	0.00
TS−Si-Pt-1H_2O	2.617	2.126	1.588	1.463		41.67 (94.92) [−51.70]	54.80
TS−Si-Pt-2H_2O	2.443	2.637	1.646	1.531	2.268	27.40	14.09
Pro−Si−Pt-H_2O	2.494	2.095	1.492	4.399		7.851	−12.03
>Ge=Pt<	2.377					0.00	0.00
TS−Ge-Pt-1H_2O	2.815	2.122	1.638	1.483		49.10 (93.65) [−43.21]	61.07
TS−Ge-Pt-2H_2O	2.540	2.859	1.700	1.544	2.402	29.56	18.32
Pro−Ge−Pt-H_2O	2.573	2.086	1.559	4.478		12.98	−5.130
>Sn=Pt<	2.549					0.00	0.00
TS−Sn-Pt-1H_2O	2.878	2.145	1.804	1.490		54.71 (93.01) [−36.17]	67.87
TS−Sn-Pt-2H_2O	2.673	2.944	1.860	1.577	2.361	30.74	38.95
Pro−Sn−Pt-H_2O	2.717	2.092	1.726	4.634		33.69	29.90
>Pb=Pt<	2.745					0.000	0.000
TS−Pb-Pt-1H_2O	3.033	2.112	1.837	1.597		58.42 (103.6) [−43.90]	70.97
TS−Pb-Pt-2H_2O	2.769	3.292	1.867	1.641	2.295	47.12	40.56
Pro−Pb−Pt-H_2O	2.810	2.073	1.773	4.616		35.06	47.93

[a]For energy surfaces, see **5**. For structures, see Figure 6. The O−H bond length in H_2O was calculated to be 0.9769 Å. [b]The values in the round bracket and the square bracket stand for $\Delta E^{\ddagger}_{strain}$ and $\Delta E^{\ddagger}_{int}$, respectively, which were obtained according to the activation strain model. See the text.

say, from both kinetic and thermodynamic viewpoints, irrespective of whether path 1 or path 2 is chosen, the lower the atomic number of the group 14 element (E) in the Bbt(Br)E=Pt(PCy_3)$_2$ complexes, the smaller is its ΔE_{st}, the lower is the activation energy and the more exothermic is the reaction for the final additional product.

We have used the activation strain model to reexamine the chemical reactions and the associated barriers.[34] Basically, the starting materials are the two separate reactants, which can approach from infinity and begin to interact as well as deform each other. As a result, the activation energy ($\Delta E^{\ddagger}$) of the transition state can be decomposed into the strain energy ($\Delta E^{\ddagger}_{strain}$) and the interaction energy ($\Delta E^{\ddagger}_{int}$). For the former, the activation strain ($\Delta E^{\ddagger}_{strain}$) is the energy associated with deforming the reactants from their equilibrium geometry into the geometry they acquire in the activated complex. On the other hand, the intrinsic interaction ($\Delta E^{\ddagger}_{int}$) is the actual interaction energy between the deformed reactants in the transition state. In consequence, one can obtain $\Delta E^{\ddagger} = \Delta E^{\ddagger}_{strain} + \Delta E^{\ddagger}_{int}$. Interested readers can find useful details in ref 34. In this work, we thus used the activation strain model to reexamine eq 3a (path 1).[35] As can be seen in Table 3, the $\Delta E^{\ddagger}_{strain}$ energy was calculated to decrease in the order (kcal/mol): 99 (**TS-C-Pt-1H_2O**) > 95 (**TS-Si-Pt-1H_2O**) > 94 (**TS-Ge-Pt-1H_2O**) ≈ 94 (**TS-Pb-Pt-1H_2O**) > 93 (**TS-Sn-Pt-1H_2O**), whereas the $\Delta E^{\ddagger}_{int}$ energy was predicted to increase in the order (kcal/mol): −69 (**TS-C-Pt-1H_2O**) < −52 (**TS-Si-Pt-1H_2O**) < −43 (**TS-Ge-Pt-1H_2O**) < −36 (**TS-Sn-Pt-1H_2O**) < −34 (**TS-Pb-Pt-1H_2O**). From these computational results, one can be understood that the trend in reactivity as shown above should be caused (at least in part) by an increasing activation strain as the E=Pt bond becomes stronger.

IV. CONCLUSION

Using DFT, this work studies the electronic structures of the Bbt(Br)E=M(PCy_2)$_2$ complexes and the Bbt(Br)E=E(Bbt)-Br molecules, as well as the mechanisms for the formation reactions for Bbt(Br)E=M(PCy_3)$_2$ and their addition reactions with water. It should be noted that this study provides the first theoretical demonstration of the reaction trajectory and the first theoretical estimation of the activation energy and reaction enthalpy for these processes. Because of the size of the systems studied in this work and in order to reduce the computational time and disk space required, the B3LYP/LANL2DZ method was used to investigate the potential energy surfaces of the reactions. Nevertheless, the electronic structures and the energies obtained at the DFT level can, at least, provide qualitatively reliable conclusions.

In summary, based on the model calculations presented here, it is readily found that the bonding character of the E=M double bond between the six valence-electron Bbt(Br)E: species and the 14 valence-electron (PCy_3)$_2$M complexes has predominantly high s-character. Namely, on the basis of the NBO, this theoretical study strongly suggests that σ-donation from the E element to the M atom prevails. Theoretical computations suggest that the relative reactivity decreases in the order: Bbt(Br)C=M(PCy_3)$_2$ > Bbt(Br)Si=M(PCy_3)$_2$ > Bbt(Br)Ge=M(PCy_3)$_2$ > Bbt(Br)Sn=M(PCy_3)$_2$ > Bbt(Br)-Pb=M(PCy_3)$_2$, irrespective of whether M = Pt or M = Pd is chosen. Namely, the greater the atomic number of the group 14 atom (E), the larger is the atomic radius of E and the more stable is its Bbt(Br)E=M(PCy_3)$_2$ doubly bonded species to chemical reactions. It is thus predicted that the Bbt(Br)Ge=M(PCy_3)$_2$, Bbt(Br)Sn=M(PCy_3)$_2$, and Bbt(Br)Pb=M-(PCy_3)$_2$ molecules should be stable and readily synthesized and isolated at room temperature. The computational results

dx.doi.org/10.1021/ic302031f | Inorg. Chem. 2013, 52, 1338−1348

can be rationalized using a simple CM model. Also, we used the activation strain model to arrive at a qualitative understanding about the 1,2-addition reactions of the Bbt(Br)E═Pt(PCy_3)$_2$ complexes with water, based on the trends in activation barriers and transition-state geometries. In consequence, not only is an explanation provided for the available experimental observations, but these approaches also provide an important insight into the factors that control doubly bonded Bbt(Br)E═M(PCy_3)$_2$ addition reactions with water and permit the prediction of the reactivity of several, as yet unknown, heavier Bbt(Br)E═M(PCy_3)$_2$ complexes.[36]

We encourage experimentalists to carry out further experiments to confirm our predictions.

■ ASSOCIATED CONTENT

Supporting Information

Table of bonding properties. Figure A: B3LYP/LANL2DZ optimized geometries (in Å and deg) of both singlet and triplet Bbt(Br)E═Pd(PCy_3)$_2$ (E = C, Si, Ge, Sn, and Pb) complexes. Figure B: calculated key molecular orbital for the singlet Bbt(Br)E═Pd(PCy_3)$_2$ (E = C, Si, Ge, Sn, and Pb) species. This material is available free of charge via the Internet at http://pubs.acs.org.

■ AUTHOR INFORMATION

Corresponding Author

*E-mail: midesu@mail.ncyu.edu.tw.

Notes

The authors declare no competing financial interest.

■ ACKNOWLEDGMENTS

The authors are grateful to the National Center for High-Performance Computing of Taiwan for generous amounts of computing time. They also thank the National Science Council of Taiwan for the financial support. Special thanks are also due to reviewers 1, 2, and 3 for very helpful suggestions and comments.

■ REFERENCES

(1) For recent reviews, see: (a) Tilley, T. D. In *The Chemistry of Organic Silicon Compounds*; Patai, S., Rappoport, Z., Eds.; Wiley: New York, 1989; Chapter 24. (b) Tilley, T. D. In *The Silicon-Heteroatom Bond*; Patai, S.; Rappoport, Z., Eds.; Wiley: New York, 1991; Chapters 9 and 10. (c) Lickiss, P. D. *Chem. Soc. Rev.* **1992**, *21*, 271. (d) Tobita, H.; Ogino, H. *Adv. Organomet. Chem.* **1998**, *42*, 223. (e) Eisen, M. S. In *The Chemistry of Organic Silicon Compounds*; Rappoport, Z., Apeloig, Y., Eds.; Wiley: New York, 1998; Chapter 35. (f) Corey, J. Y.; Braddock-Wilking, J. *Chem. Rev.* **1999**, *99*, 175. (g) Gehrhus, B.; Lappert, M. F. J. *Organomet. Chem.* **2001**, *617*−*618*, 209. (h) Ogino, H. *Chem. Rec.* **2002**, *2*, 291. (i) Okazaki, M.; Tobita, H.; Ogino, H. *Dalton Trans.* **2003**, 494. (j) Hill, N. J.; West, R. J. *Organomet. Chem.* **2004**, *689*, 4165. (k) For reviews on silylene-transition metal complexes, see: Waterman, R.; Hayes, P. G.; Tilley, T. D. *Acc. Chem. Res.* **2007**, *40*, 712 and related references therein. (l) for reviews on carbene-transition metal complexes, see: de Frémont, P.; Marion, N.; Nolan, S. P. *Coord. Chem. Rev.* **2009**, *253*, 862 and related references therein. (m) Corey, J. Y. *Chem. Rev.* **2011**, *111*, 863.

(2) For instance, see: (a) (i) Herrmann, W. A.; Denk, M.; Behrn, J.; Scherer, W.; Klingan, F.-R.; Bock, H.; Solouki, B.; Wagner, M. *Angew. Chem.* **1992**, *104*, 1489. (b) Gehrhus, B.; Hitchcock, P. B.; Lappert, M. F.; Maciejewski, H. *Organometallics* **1998**, *17*, 5599. (c) Schmedake, T. A.; Haaf, M.; Paradise, B. J.; Powell, D.; West, R. *Organometallics* **2000**, *19*, 3263. (d) Schmedake, T. A.; Haaf, M.; Paradise, B. J.; Millevolte, A. J.; Powell, D. R.; West, R. *J. Organomet. Chem.* **2001**, *636*, 17. (e) Fürstner, A.; Krause, H.; Lehmann, C. W. *Chem. Commun.* **2001**, 2372. (f) Herrmann, W. A.; Härter, P.; Gstöttmayr, C. W. K.; Bielert, F.; Seeboth, N.; Sirsch, P. *J. Organomet. Chem.* **2002**, *649*, 141. (g) Avent, A. G.; Gehrhus, B.; Hitchcock, P. B.; Lappert, M. F.; Maciejewski, H. *J. Organomet. Chem.* **2003**, *686*, 321. (h) Kühl, O.; Lönnecke, P.; Heinicke, J. *Inorg. Chem.* **2003**, *42*, 2836. (i) Neumann, E.; Pfaltz, A. *Organometallics* **2005**, *24*, 2008. (j) Zeller, A.; Bielert, F.; Haerter, P.; Herrmann, W. A.; Strassner, T. *J. Organomet. Chem.* **2005**, *690*, 3292. (k) Jutzi, P.; Leszczynska, L.; Mix, A.; Neumann, B.; Rummel, B.; Schoeller, W.; Stammler, H.-G. *Organometallics* **2010**, *29*, 4759. (l) Sheu, J.-H.; Su, M.-D. *Organometallics* **2012**, *31*, 3101.

(3) Inoue, S.; Driess, M. *Organometallics* **2009**, *28*, 5032.

(4) Agou, T.; Sasamori, T.; Tokitoh, N. *Organometallics* **2012**, *31*, 1150.

(5) For earlier publications on >E═[M] double bonds, for instance, see: (a) Jacobsen, H.; Ziegler, T. *J. Am. Chem. Soc.* **1994**, *116*, 3667. (b) Radius, U.; Bickelhaupt, F. M. *Coord. Chem. Rev.* **2009**, *253*, 678. (c) Jacobsen, H.; Correa, A.; Poater, A.; Costabile, C.; Cavallo, L. *Coord. Chem. Rev.* **2009**, *253*, 687.

(6) It has to be mentioned here that the motivation for this work is stimulated by and/or originated from the knowledge on the recent progress in the chemistry of 1,2-dihalodimetallenes and related compounds reported by Tokitoh et al. See ref 4 and references therein. The reason for selecting the substituent, Bbt, does not imply that other bulky groups are not important. It means only that we acknowledge that the size of the systems currently studied prevents highly accurate optimizations in the quantum theoretical calculations and we also know that the Bbt group is a quite useful and widespread substituent. We thus choose the Bbt substituent to treat such metallylene-transitioin metal species using the B3LYP/LANL2DZ level of theory. In view of recent dramatic developments in metallylene-transitioin metal chemistry, it is therefore hoped that our theoretical study will provide a crucial starting point for developing metallylene and transitioin metal doubly bonded molecules and for opening up new synthetic areas.

(7) (a) Becke, A. D. *Phys. Rev. A* **1988**, *38*, 3098. (b) Becke, A. D. *J. Chem. Phys.* **1993**, *98*, 5648.

(8) Lee, C.; Yang, W.; Parr, R. G. *Phys. Rev. B* **1988**, *37*, 785.

(9) (a) Su, M.-D. *J. Phys. Chem. A* **2004**, *108*, 823. (b) Su, M.-D. *Inorg. Chem.* **2004**, *43*, 4846. (c) Su, M.-D. *Eur. J. Chem.* **2004**, *10*, 6073 and related references therein..

(10) (a) Hay, P. J.; Wadt, W. R. *J. Chem. Phys.* **1985**, *82*, 270;(b) *J. Chem. Phys.* **1985**, *82*, 284;(c) *J. Chem. Phys.* **1985**, *82*, 299. (d) Check, C. E.; Faust, T. O.; Bailey, J. M.; Wright, B. J.; Gilbert, T. M.; Sunderlin, L. S. *J. Phys. Chem. A* **2001**, *105*, 8111.

(11) Dunning, T. H., Jr.; Hay, P. J. In *Modern Theoretical Chemistry*, Schaefer, H. F., III, Ed.; Plenum: New York, 1976; pp 1−28.

(12) Glendening, E. D.; Reed, A. E.; Carpenter, J.; Weinhold, F. *NBO*, Version 3.1; University of Wisconsin-Madison: Madison, WI, 1992.

(13) Wiberg, K. B. *Tetrahedron* **1968**, 1083.

(14) Frisch, M. J.; Trucks, G. W.; Schlegel, H. B.; Scuseria, G. E.; Robb, M. A.; Cheeseman, J. R.; Zakrzewski, V. G.; Montgomery, Jr., J. A.; Vreven, T.; Kudin, K. N.; Burant, J. C.; Millam, J. M.; Iyengar, S. S.; Tomasi, J.; Barone, V.; Mennucci, B.; Cossi, M.; Scalmani, G.; Rega, N.; Petersson, G. A.; Nakatsuji, H.; Hada, M.; Ehara, M.; Toyota, K.; Fukuda, R.; Hasegawa, J.; Ishida, M.; Nakajima, T.; Honda, Y.; Kitao, O.; Nakai, H.; Klene, M.; Li, X.; Knox, J. E.; Hratchian, H. P.; Cross, J. B.; Adamo, C.; Jaramillo, J.; Gomperts, R.; Stratmann, R. E.; Yazyev, O.; Austin, A. J.; Cammi, R.; Pomelli, C.; Ochterski, J. W.; Ayala, P. Y.; Morokuma, K.; Voth, G. A.; Salvador, P.; Dannenberg, J. J.; Zakrzewski, V. G.; Dapprich, S.; Daniels, A. D.; Strain, M. C.; Farkas, O.; Malick, D. K.; Rabuck, A. D.; Raghavachari, K.; Foresman, J. B.; Ortiz, J. V.; Cui, Q.; Baboul, A. G.; Clifford, S.; Cioslowski, J.; Stefanov, B. B.; Liu, G.; Liashenko, A.; Piskorz, P.; Komaromi, I.; Martin, R. L.; Fox, D. J.; Keith, T.; Al-Laham, M. A.; Peng, C. Y.; Nanayakkara, A.; Challacombe, M.; Gill, P. M. W.; Johnson, B.; Chen, W.; Wong, M. W.; Gonzalez, C.; Pople, J. A. Gaussian, Inc.: Wallingford, CT, 2003.

(15) Lowry, T. H.; Richardson, K. S. In *Mechanism and Theory in Organic Chemistry*, 3rd Ed.; HarperCollins Publishers: New York, 1987; pp 546−562.
(16) Su, M.-D.; Chu, S.-Y. *Inorg. Chem.* **1998**, *37*, 3400.
(17) Albright, T. A.; Burdett, J. K.; Whangbo, M. H. In *Orbital Interaction in Chemistry*; Wiley: New York, 1985; Chapter 2.
(18) The dihedral angle θ (deg) is between the coordination planes of the low-coordinated silicon (defined by Si, Pt, C and Br atoms) and platinum (Pt, Si, the two P atoms). See Figure 2.
(19) The atomic radius for group 14 elements and platinum are as follows: C (0.77), Si (1.17 Å), Ge (1.22 Å), Sn (1.40 Å), Pb (1.54 Å), and Pt (1.30 Å). Also see ref 4.
(20) (a) Pyykkö, P.; Desclaux, J.-P. *Acc. Chem. Res.* **1979**, *12*, 276. (b) Kutzelnigg, W. *Angew. Chem., Int. Ed. Engl.* **1984**, *23*, 272. (c) Pyykkö, P. *Chem. Rev.* **1988**, *88*, 563. (d) Pyykkö, P. *Chem. Rev.* **1997**, *97*, 597.
(21) For instance: (a) Raabe, G.; Michl, J. *Chem. Rev.* **1985**, *85*, 419. (b) Brook, A. G.; Baines, K. M. *Adv. Organomet. Chem.* **1986**, *25*, 1. (c) West, R. *Angew. Chem., Int. Ed.* **1987**, *26*, 1201. (d) Tsumuraya, T.; Batcheller, S. A.; Masamune, A. *Angew. Chem., Int. Ed.* **1991**, *30*, 902. (e) Wade, Jr. L. G. In *Organic Chemistry*; Pearson Education Inc.: New York, 2009; p 282.
(22) For instance: (a) West, R.; Fink, M. J.; Michl, J. *Science* **1981**, *214*, 1343. (b) Masamune, S.; Hanzawa, Y.; Murakami, S.; Bally, T.; Blount, J. F. *J. Am. Chem. Soc.* **1982**, *104*, 1150. (c) Sasamori, T.; Hironaka, K.; Sugiyama, Y.; Takagi, N.; Nagase, S.; Hosoi, Y.; Furukawa, Y.; Tokitoh, N. *J. Am. Chem. Soc.* **2008**, *130*, 13856.
(23) For instance: (a) Hitchcock, P. B.; Lappert, M. F.; Miles, S. J.; Thorne, A. J. *Chem. Commun.* **1984**, 480. (b) Snow, J. T.; Murakami, S.; Masamune, S.; Williams, D. J. *Tetrahedron Lett.* **1984**, *25*, 4191. (c) Goldberg, D. E.; Hitchcock, P. B.; Lappert, M. F.; Thomas, K. M.; Thorne, A. J.; Fjelberg, T.; Haaland, A.; Schilling, B. E. R. *Dalton Trans.* **1986**, 2387. (d) Sasamori, T.; Sugiyama, Y.; Takeda, N.; Tokitoh, N. *Organometallics* **2005**, *24*, 3309.
(24) For instance: (a) Lay, U.; Pritzkow, H.; Grützmacher, H. *Chem. Commun.* **1992**, 260. (b) Weidenbruch, M.; Kilian, H.; Peters, H.; Schnering, H. G. V.; Marsmann, H. *Chem. Ber.* **1995**, *128*, 983. (c) Klinkhammer, K. W.; Schwarz, W. *Angew. Chem., Int. Ed.* **1995**, *34*, 1334. (d) Leung, W. P.; Kwok, W.-H.; Xue, F.; Mak, T. C. W. *J. Am. Chem. Soc.* **1997**, *119*, 1145.
(25) For instance: (a) Stürmann, M.; Weidenbruch, M.; Klinkhammer, K. W.; Lissner, F.; Marsmann, H. *Organometallics* **1998**, *17*, 4425. (b) Stürmann, M.; Saak, W.; Weidenbruch, M.; Klinkhammer, K. W. *Eur. J. Inorg. Chem.* **1999**, 579. (c) Stürmann, M.; Saak, W.; Marsmann, H.; Weidenbruch, M. *Angew. Chem., Int. Ed.* **1999**, *38*, 187.
(26) Su, M.-D. *J. Phys. Chem.* **1996**, *100*, 4339 and related references therein.
(27) For recent reviews, see: (a) Grev, R. S. *Adv. Organomet. Chem.* **1991**, *33*, 125. (b) Esoudie, J.; Couret, C.; Ranaivonjatovo, H.; Satge, J. *Coord. Chem. Rev.* **1994**, *130*, 427. (c) Driess, M. *Coord. Chem. Rev.* **1995**, *145*, 1. (d) Mackay, K. M. in *The Chemistry of Organic Germanium, Tin, and Lead Compounds*; Patai, S., Ed.; Wiley: Chichester, U.K., 1995; Chapter 4. (e) Klinkhammer, K. W. *Angew. Chem., Int. Ed. Engl.* **1997**, *36*, 2320. (f) Barrau, J.; Rina, G. *Coord. Chem. Rev.* **1998**, *178*, 593. (g) Power, P. P. *J. Chem. Soc., Dalton Trans.* **1998**, 2939. (h) Tokitoh, N.; Matsumoto, T.; Okazaki, R. *Bull. Chem. Soc. Jpn.* **1999**, *72*, 1665. (i) Robinson, G. H. *Acc. Chem. Res.* **1999**, *32*, 773. (j) Power, P. P. *Chem. Rev.* **1999**, *99*, 3463. (k) Leigh, W. J. *Pure Appl. Chem.* **1999**, *71*, 453. (l) Tokitoh, N. *Pure Appl. Chem.* **1999**, *71*, 495. (m) Gruetzmacher, H.; Fassler, T. F. *Chem.—Eur. J.* **2000**, *6*, 2317. (n) Kira, M.; Iwamoto, T. *J. Organomet. Chem.* **2000**, *610*, 236. (o) Tokitoh, N.; Okazaki, R. *Coord. Chem. Rev.* **2000**, *210*, 251. (p) Malcolm, N. O. J.; Gillespie, R. J.; Popelier, P. L. A. *J. Chem. Soc., Dalton Trans.* **2002**, 3333. (q) Tokitoh, N.; Okazaki, R. *The Chemistry of Organic Germanium, Tin and Lead Compounds*; Rappoport, Z., Ed.; Wiley: Chichester, 2002; *Vol. 2*, Chapter 13. (r) Klinkhammer, K. W. *The Chemistry of Organic Germanium, Tin and Lead Compounds*; Rappoport, Z., Ed.; Wiley: Chichester, 2002; Vol. 2, Chapter 4. (s) Lee, V. Y.; Sekiguchi, A. *Organometallics* **2004**, *23*, 2822. (t) Schleyer, P. v. R. *The Chemistry of Organic Silcon Compounds*; Rappoport, Z., Apeloig, Y., Eds.; John Wiley & Sons: London, 2001; pp 1−163 and reference therein.
(28) Albright, T. A.; Burdett, J. K.; Whangbo, M.-H., *Orbital Interactions in Chemistry*; John Wiley & Sons: New York, 1985; p 164.
(29) For instance, see: (a) Zilm, K. W.; Lawless, G. A.; Merrill, R. M.; Miller, J. M.; Webb, G. G. *J. Am. Chem. Soc.* **1987**, *109*, 7236. (b) Tokitoh, N.; Suzuki, H.; Okazaki, R. *J. Am. Chem. Soc.* **1993**, *115*, 10428. (c) Pu, L. H.; Olmstead, M. M.; Power, P. P.; Schiemenz, B. *Organometallics* **1998**, *17*, 5602. (d) Bona, M. A.; Cassani, M. C.; Keates, J. M.; Lawless, G. A.; Lappert, M. F.; Sturmann, M.; Weidenbruch, M. *Dalton Trans.* **1998**, 1187. (e) Kishikawa, K.; Tokitoh, N.; Okazaki, R. *Chem. Lett.* **1998**, 239. (f) Pu, L. H.; Phillips, A. D.; Richards, A. F.; Stender, M.; Simons, R. S.; Olmstead, M. M.; Power, P. P. *J. Am. Chem. Soc.* **2003**, *125*, 11626.
(30) For instance, see: (a) Simons, R. S.; Pu, L.; Olmstead, M. M.; Power, P. P. *Organometallics* **1997**, *16*, 1920. (b) Power, P. P. *J. Chem. Soc., Dalton Trans.* **1998**, 2939. (c) Stender, M.; Pu, L. H.; Power, P. P. *Organometallics* **2001**, *20*, 1820.
(31) For instance, see: (a) Suzuki, K.; Matsuo, T.; Hashiznme, D.; Tamao, K. *J. Am. Chem. Soc.* **2011**, *133*, 19710. (b) Mizuhata, Y.; Sasamori, T.; Tokitoh, N. *Chem. Rev.* **2009**, *109*, 3479.
(32) For details, see: (a) Shaik, S.; Schlegel, H. B.; Wolfe, S. In *Theoretical Aspects of Physical Organic Chemistry*; John Wiley & Sons Inc.: New York, 1992. (b) Pross, A. In *Theoretical and Physical Principles of Organic Reactivity*; John Wiley & Sons Inc.: New York, 1995. (c) Shaik, S. *Prog. Phys. Org. Chem.* **1985**, *15*, 197. (d) Shaik, S.; Hiberty, P. C. In *A Chemist's Guide to Valence Bond Theory*; Wiley, Interscience, New York, 2008.
(33) (a) The first paper that originated the CM model see: Shaik, S. *J. Am. Chem. Soc.* **1981**, *103*, 3692. (b) About the most updated review of the CM model, one can see: Shaik, S.; Shurki, A. *Angew. Chem., Int. Ed.* **1999**, *38*, 586.
(34) For the activation strain model, for instance, see: (a) Bickelhaupt, F. M. *J. Comput. Chem.* **1999**, *20*, 114. (b) de Jong, G. T.; Bickelhaupt, F. M. *ChemPhysChem* **2007**, *8*, 1170. (c) van Zeist, W.-J.; Bickelhaupt, F. M. *Org. Biomol. Chem.* **2010**, *8*, 3118 and related references therein.
(35) Since we have the equilibrium geometries of the reactant fragments (Bbt(Br)E═Pt$(PCy_3)_2$ fragment + H_2O) as well as their deformed geometries in the transition states. Then, $\Delta E^{\ddagger}_{strain}$ = E(deformed fragments) − E(optimized fragments) and $\Delta E^{\ddagger}_{int} = \Delta E^{\ddagger} - \Delta E^{\ddagger}_{strain}$. The results of the analyses are given in Table 3.
(36) The approaches (the CM model and the activation strain model) we used in the present study, in spite of their simplicity, can provide chemists with important insights into the factors controlling these chemical reactions, and thus permit them to predict the reactivity of some unknown doubly bonded (Bbt(Br)E═M$(PCy_3)_2$ species. For one useful reference, see: Hoffmann, R.; Schleyer, P. R.; Schaefer, H. F. *Angew. Chem. Int. Ed.* **2008**, *47*, 7164.